ETH
Eidgenössische Technische Hochschule Zürich
Swiss Federal Institute of Technology Zurich

Seminar for Applied Mathematics SAM

Spectral convergence of defect modes in large finite resonator arrays

H. Ammari and B. Davies and E.O. Hiltunen

Research Report No. 2023-05
January 2023

Seminar für Angewandte Mathematik
Eidgenössische Technische Hochschule
CH-8092 Zürich
Switzerland

Spectral convergence of defect modes in large finite resonator arrays

Habib Ammari* Bryn Davies† Erik Orvehed Hiltunen‡

Abstract

We show that defect modes in infinite systems of resonators have corresponding modes in finite systems which converge as the size of the system increases. We study the generalized capacitance matrix as a model for three-dimensional coupled resonators with long-range interactions and consider defect modes that are induced by compact perturbations. If such a mode exists, then there are elements of the discrete spectrum of the corresponding truncated, finite system converging algebraically to each element of the pure point spectrum. This result, which concerns periodic lattices of arbitrary dimension in a three-dimensional differential system, is in contrast with the exponential convergence observed in one-dimensional problems. This is due to the presence of long-range interactions in the system, which gives a dense matrix model and shows that exponential convergence cannot be expected in physical systems.

Mathematics Subject Classification (MSC2010): 35J05, 35C20, 35P20.

Keywords: finite crystals, metamaterials, edge effects, capacitance coefficients, subwavelength resonance

1 Introduction

Much of the physical literature concerning wave propagation in periodic media relies on a believable but highly non-trivial piece of logic. That is, researchers want to be able to relate the spectral properties of infinite periodic structures with truncated, finite versions of the same material. The motivation for this is that infinite periodic structures can be described very concisely using Floquet-Bloch analysis [12]. However, finite, truncated versions of the structure are often required when it comes to either numerical or physical experiments. It is perfectly plausible that the two structures should behave similarly, particularly away from the edges of the truncated structure and especially when the truncated structure is very large. However, a precise convergence theory relating the spectra of these two quite different differential operators is, in general, yet to be developed.

The many interesting phenomena that occur at the edges of periodic arrays have been studied in some detail [10]. For example, there is a tendency for wave energy to be localized to the edges of the structure, taking the form of surface waves [15, 20]. This is an example of an *edge effect* and highlights that there will always be fundamental differences between how infinite and truncated structures interact with waves. Another important question that has been explored in this field, and is intimately related to the results presented in this work, is the extent to which waves incident on the edge of a truncated periodic structure can excite Bloch waves in the structure (thus, replicating the behaviour of its infinite counterpart) [11, 18, 19].

The central question of this work is the extent to which the resonant spectra of infinite and truncated structures can be related. We will focus on localized modes which decay quickly outside of some compact region, meaning they are less severely affected by edge effects. Additionally, localized modes are the eigenmodes of interest for many wave guiding applications. Existing results have shown that in certain one-dimensional systems, any *defect mode* of the infinite structure will have a corresponding

*Department of Mathematics, ETH Zurich, Zurich, Switzerland (habib.ammari@math.ethz.ch).
†Department of Mathematics, Imperial College London, London, UK (bryn.davies@imperial.ac.uk).
‡Department of Mathematics, Yale University, New Haven, USA (erik.hiltunen@yale.edu).

mode in the truncated structure converging to the defect mode as the size tends to infinity [13, 14, 16]. A defect mode is a mode that is created by making a perturbation to introduce a defect to the periodic structure. Such a mode is characterized by being spatially localized (in the sense that it decays quickly enough to be square integrable along the axis or axes of periodicity) and having an eigenfrequency that belongs to the pure point spectrum of the perturbed periodic operator. The terminology "pure point spectrum" and "defect mode eigenfrequency" are preferred by spectral analysts and wave physicists, respectively, and we will use them somewhat interchangeably here. The rest of the spectrum will typically be composed of the *continuous spectrum*, which corresponds to the Bloch modes that propagate through the material without decaying.

In previous works, it was shown that the convergence of defect mode eigenfrequency to the pure point spectrum of the infinite periodic operator was exponential with respect to the size of the truncated array [13, 14, 16]. These results concerned one-dimensional systems (or, equivalently, tridiagonal matrix models). In this work, we study the *generalized capacitance matrix*, which is a dense resonator model that includes long-range interactions [1]. We will recall how this model can be derived from a three-dimensional scattering problem with high-contrast resonators. However, it can be viewed more generally as a canonical model for coupled resonators. In this setting, we will prove that any defect mode eigenfrequency of the infinite structure has a sequence of eigenvalues of the truncated structures converging to it. However, in contrast to the one-dimensional and tridiagonal models explored previously, we observed that this convergence is algebraic. This occurs due to the structure of the problem and is an inherent consequence of the density of the matrix model. We believe that similar behaviour will be observed in other multi-dimensional differential systems and dense matrix models.

This paper is split into three main parts. In Section 2, we introduce the matrix model (the generalized capacitance matrix) that we will study and prove some elementary properties that lay the foundations for the subsequent analysis. Section 3 contains the main results of this work, which show that the truncated structures have eigenfrequencies that converge to the pure point spectrum of the infinite structure. Finally, in Section 4, we present numerical evidence for the convergence of the truncated spectra to the continuous spectrum. Proving convergence to these Bloch modes remains an open problem; however, the constructive nature of the generalized capacitance matrix approach presented in this work provides a promising platform for future investigations.

2 The generalized capacitance matrix model

In this section, we will introduce the generalized capacitance matrix model that will be the object of this study. Its definition uses layer potentials to capture the (potentially complex) shapes of the resonators. In Appendix A we briefly present asymptotic results showing how this model can be deduced from a subwavelength resonance problem with a system of high-contrast resonators. Finally, we will prove a convergence result for the capacitance coefficients that will be the basis of the theorems in subsequent sections.

2.1 Definition

We study a system of periodically repeated resonators in a lattice in $\mathbb{R}^3$. We take lattice vectors $l_1, \dots, l_d \in \mathbb{R}^3$, where $0 < d < 3$, and let Λ denote the lattice generated by these vectors. In other words,

$$\Lambda := \{m_1 l_1 + \cdots + m_d l_d \mid m_i \in \mathbb{Z}\}.$$

At this point, we remark that there are three possible cases: $d = 1$, corresponding to a *chain* of resonators; $d = 2$, corresponding to a *screen* of resonators; or $d = 3$, corresponding to a *crystal* of resonators. For simplicity, we assume that the lattice is aligned with the first d coordinate axes.

We take $Y \subset \mathbb{R}^3$ to be a single unit cell,

$$Y = \begin{cases} \{c_1 l_1 + x_2 e_2 + x_3 e_3 \mid 0 \le c_1 \le 1, x_2, x_3 \in \mathbb{R}\}, & d = 1, \\ \{c_1 l_1 + c_2 l_2 + x_3 e_3 \mid 0 \le c_1, c_2 \le 1, x_3 \in \mathbb{R}\}, & d = 2, \\ \{c_1 l_1 + c_2 l_2 + c_3 l_3 \mid 0 \le c_1, c_2, c_3 \le 1\}, & d = 3. \end{cases}$$

We let $D \subset Y$ be a collection of N resonators contained in Y

$$D = \bigcup_{i=1}^{N} D_i,$$

where D_n are disjoint domains in Y with boundary $\partial D_i \in C^{1,s}$ for $s > 0$. In the periodic lattice, we let $D_i^m = D_i + m$, for $m \in \Lambda$, and then denote the full lattice as

$$\mathcal{D} = \bigcup_{m\in\Lambda} \bigcup_{i=1}^{N} D_i^m.$$

We will define a finite system of resonators resulting from truncation of the periodic lattice. Let $I_r \subset \Lambda$ be all lattice points within distance r from the origin

$$I_r = \{m \in \Lambda \mid |m| < r\}.$$

We define the finite collection of resonators $\mathcal{D}_{\mathrm{f}} = \mathcal{D}_{\mathrm{f}}(r)$ as

$$\mathcal{D}_{\mathrm{f}}(r) = \bigcup_{m\in I_r} D + m.$$

In this setting, $\mathcal{D}_{\mathrm{f}}$ is a finite lattice where D is the single, repeated unit. The goal is to clarify in which sense the spectral properties of a finite, but large, lattice can be approximated by the corresponding infinite one.

We let G be the Green's function for Laplace's equation in three dimensions:

$$G(x) = -\frac{1}{4\pi|x|}.$$

Given a bounded domain $\Omega \subset \mathbb{R}^3$, we then define the *single layer potential* $\mathcal{S}_\Omega : L^2(\partial\Omega) \to H^1(\partial\Omega)$ as

$$\mathcal{S}_\Omega[\varphi](x) := \int_{\partial\Omega} G(x-y)\varphi(y)\,\mathrm{d}\sigma(y), \quad x \in \partial\Omega.$$

Specifically, $\mathcal{S}_\Omega$ is known to be invertible [7]. For a finite lattice, we define the capacitance coefficients as

$$(C_{\mathrm{f}}^{mn})_{ij}(r) = \int_{\partial D_i^m} \mathcal{S}_{\mathcal{D}_{\mathrm{f}}}^{-1}[\chi_{\partial D_j^n}]\,\mathrm{d}\sigma, \tag{2.1}$$

for $1 \le i,j \le N$ and $m,n \in I_r$. Here, we explicitly indicate the dependence of the size r of the truncated lattice. For $m,n \in I_r$, we observe that $C_{\mathrm{f}}^{mn}(r)$ is a matrix of size $N \times N$, while the block matrix $C_{\mathrm{f}} = (C_{\mathrm{f}}^{mn})$ is a matrix of size $N|I_r| \times N|I_r|$.

We next define the capacitance coefficients for the infinite lattice. We begin by defining the dual lattice Λ^* of Λ as the lattice generated by $\alpha_1, ..., \alpha_d$ satisfying $\alpha_i \cdot l_j = 2\pi\delta_{ij}$ and $P_\perp \alpha_i = 0$, for $i,j = 1, ..., d$. We define the *Brillouin zone* Y^* as $Y^* := \big(\mathbb{R}^d \times \{\mathbf{0}\}\big)/\Lambda^*$, where $\mathbf{0}$ is the zero-vector in $\mathbb{R}^{3-d}$. We remark that Y^* can be written as $Y^* = Y_d^* \times \{\mathbf{0}\}$, where Y_d^* has the topology of a torus in d dimensions.

When $\alpha \notin Y \setminus \{0\}$, we can define the quasi-periodic Green's function $G^\alpha(x)$ as

$$G^\alpha(x) := \sum_{m\in\Lambda} G(x-m)e^{\mathrm{i}\alpha\cdot m}. \tag{2.2}$$

The series in (2.2) converges uniformly for x and y in compact sets of $\mathbb{R}^d$, with $x \neq y$ and $\alpha \neq 0$. Given a bounded domain $\Omega \subset Y$, we can then define the *quasi-periodic* single layer potential $\mathcal{S}_\Omega^\alpha : L^2(\partial\Omega) \to H^1(\partial\Omega)$ as

$$\mathcal{S}_\Omega^\alpha[\varphi](x) := \int_{\partial\Omega} G^\alpha(x-y)\varphi(y)\,\mathrm{d}\sigma(y), \quad x \in \partial\Omega. \tag{2.3}$$

For $\alpha \in Y^*$ and for $1 \le i,j \le N$, the quasi-periodic capacitance matrix ("dual-space" representation) is the $N \times N$-matrix defined as

$$\widehat{C}_{ij}^\alpha = \int_{\partial D_i} (\mathcal{S}_D^\alpha)^{-1}[\chi_{\partial D_j}]\,\mathrm{d}\sigma. \tag{2.4}$$

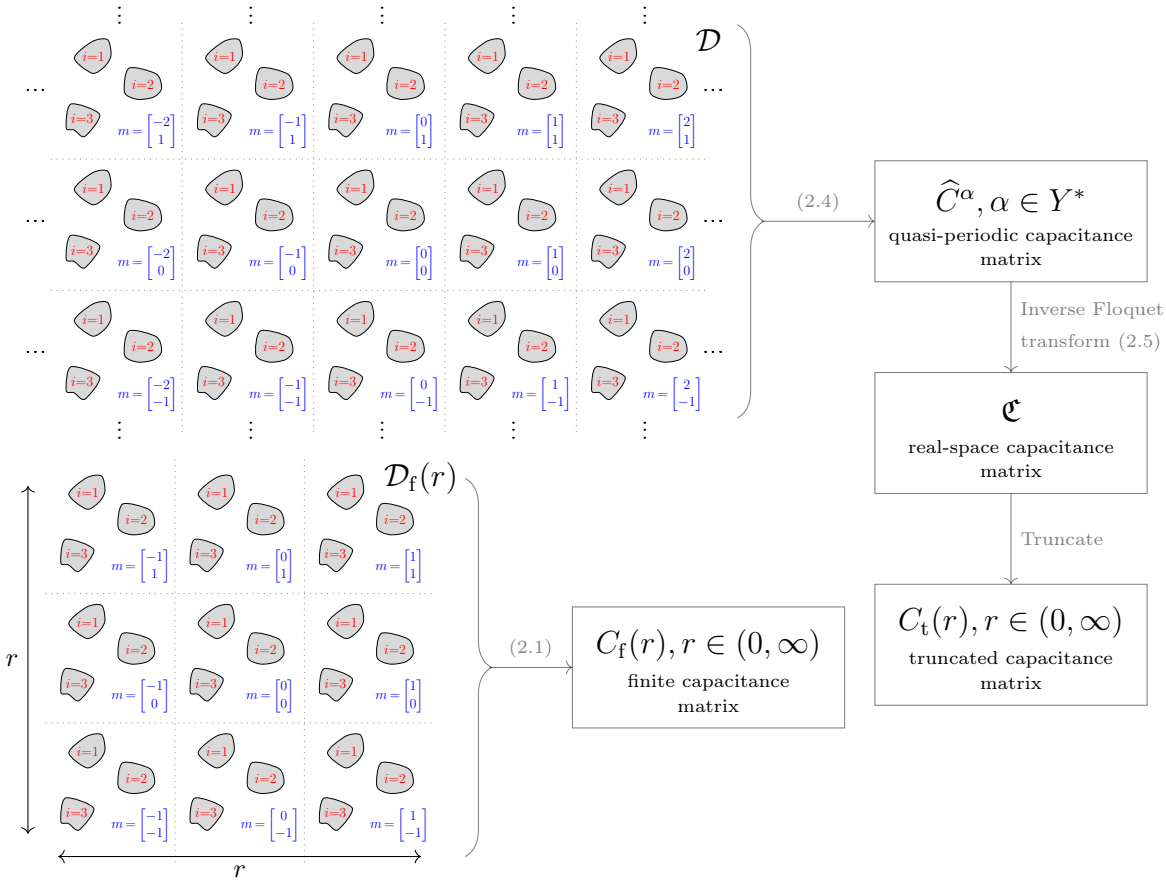

Figure 1: This work studies the convergence of the eigenfrequencies of defect modes in a truncated periodic material to the spectrum of the corresponding infinite material. We use capacitance matrices as a canonical model for many-body scattering of time-harmonic waves. The aim of this work is to show how eigenvalues of the finite capacitance matrix $C_\mathrm{f}(r)$ converge to those of the real-space capacitance matrix $\mathfrak{C}$. The calligraphic font for $\mathfrak{C}$ denotes the fact that this is an infinite matrix. Our strategy is to compare the spectrum of $C_\mathrm{f}(r)$ with the truncated capacitance matrix $C_\mathrm{t}(r)$, which is obtained by truncating all but a finite $O(r)$ number of rows in $\mathfrak{C}$, before letting $r \to \infty$. Throughout this work, we use the block matrix notation $(C^{mn})_{ij}$ to refer to the $i,j \in \{1,\dots,N\}$ entry of the $n,m \in \Lambda$ block in a matrix C.

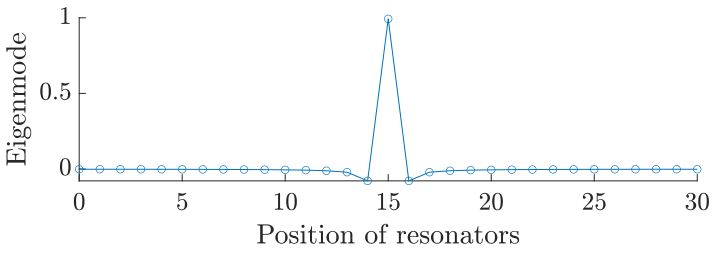

Figure 2: An example of a localized defect mode for a system of 31 resonators. The eigenvalues of the finite matrix $B_{\mathrm{t}}C_{\mathrm{f}}$ are computed, where C_{f} is the generalized capacitance matrix for a system of evenly spaces resonators and B_{t} is the identity matrix but with the central entry $(B_{\mathrm{t}})^0_{11} = 2$.

For $1 \leq i, j \leq N$, we can then define the "real-space" capacitance coefficients at the lattice point m by

$$C_{ij}^m = \frac{1}{|Y^*|} \int_{Y^*} \widehat{C}_{ij}^{\alpha} e^{-\mathrm{i}\alpha\cdot m} \, \mathrm{d}\alpha. \tag{2.5}$$

Here, C_{ij}^0 corresponds to the diagonal block which contains the capacitance coefficients of the resonators within a single unit cell. We use the notation $\mathfrak{C}$ to denote the infinite matrix that contains all the C_{ij}^m coefficients, for all $1 \leq i, j \leq N$ and all $m \in \Lambda$.

A final, important quantity for the analysis in this work is the truncated capacitance matrix C_{t}. This is obtained by keeping only $N|I_r| \times N|I_r|$ coefficients from $\mathfrak{C}$, to give a matrix that is the same size as C_{f}. A schematic of the various pieces of notation used in this article and how they related to each other is given in Figure 1. The proof strategy deployed in this work is to compare the spectra of C_{f} with that of C_{t}, and then let $r \to \infty$ in order to approximate the spectrum of $\mathfrak{C}$. In particular, the modes that we will compare are *defect modes*, which are spatially localized modes that exist due to the presence of defects in the otherwise periodic material, an example of which is shown in Figure 2.

We will model defect modes through pre-multiplication by a defect matrix $\mathfrak{B}$. For each $m \in \Lambda$, we let B^m be an $N \times N$ diagonal matrix

$$B^m = \begin{pmatrix} b_1^m & 0 & \cdots & 0 \\ 0 & b_2^m & \cdots & 0 \\ \vdots & \vdots & \ddots & \vdots \\ 0 & 0 & \cdots & b_N^m \end{pmatrix}, \tag{2.6}$$

where the diagonal entries b_i^m are real-valued parameters. In this work, we only consider *compact* defects, where $b_i^m = 1$ for all but finitely many i and m. For the infinite structure, we let $\mathfrak{B}$ be the infinite block-diagonal matrix that contains B^m for all $m \in \Lambda$. Under the assumption on the b_i^m, $\mathfrak{B}$ is said to be a compact perturbation of the identity. The spectrum of the infinite structure is given by the solutions to the spectral problem

$$\mathfrak{B}\mathfrak{C}\mathfrak{u} = \lambda \mathfrak{u}. \tag{2.7}$$

For the finite structure of size r, we let B_{t} be the block-diagonal matrix $(B^m), m \in I_r$ and consider the spectral problem

$$B_{\mathrm{t}}C_{\mathrm{f}}u = \lambda u.$$

An example of such a defect mode is shown in Figure 2. A system of 31 resonators is modelled, with the finite defect matrix B_{t} chosen to be the identity, perturbed so that its central element is $(B_{\mathrm{t}})^0_{11} = 2$.

The generalized capacitance matrix serves not only as a canonical model for coupled resonators (whose interaction terms decay as r^{-1}), but can also be derived from first principles in certain physical settings. For example, in Appendix A we briefly explain how this model arises for a system of high-contrast resonators in which case the eigenstates of the generalized capacitance matrix fully characterize the subwavelength resonant spectrum of the system.

2.2 Convergence of capacitance coefficients

Based on the layer-potential characterization of capacitance, we prove in this section that the capacitance coefficients of a large but finite structure converge, as the size grows, to corresponding coefficients

of the infinite structure. We begin with the following result, which collects some well-known results on the capacitance matrices [1, 8].

Lemma 2.1. *Let $\widehat{C}^\alpha$ and C_f be the quasi-periodic and finite capacitance matrix, respectively. Then*

(i) $\widehat{C}^\alpha$ and C_f are symmetric, positive definite matrices;

(ii) $\widehat{C}^\alpha$ and C_f are strictly diagonally dominant matrices;

(iii) We have $(\widehat{C}^\alpha)_{ii} > 0$ and $(C_\mathrm{f}^{mm})_{ii} > 0$. Moreover, for $i \neq j$ and $m \neq n$ we have $(\widehat{C}^\alpha)_{ij} < 0$ and $(C_\mathrm{f}^{mn})_{ij} < 0$.

The next result shows that a fixed block of the infinite capacitance matrix is approximately equal to corresponding block of the capacitance matrix of the finite structure. In other words, the finite-structure capacitance coefficients can be approximated through the infinite structure as long as we are sufficiently far away from the edges of the finite structure.

Theorem 2.2. *For fixed $m, n \in \Lambda$, we have as $r \to \infty$,*

$$\lim_{r\to\infty} C_\mathrm{f}^{mn}(r) = C^{m-n}.$$

Proof. Firstly, observe that

$$\mathcal{S}_{\mathcal{D}_\mathrm{f}}[\psi] = \sum_{m\in I_r} \mathcal{S}_{D+m}[\psi_m],$$

where $\psi_m = \psi|_{\partial D+m}$. Recall that the quasi-periodic single-layer potential is defined as

$$\mathcal{S}_D^\alpha[\phi] = \int_{\partial D} \sum_{m\in\Lambda} G(x-y-m)e^{\mathrm{i}\alpha\cdot m}\phi(y)\,\mathrm{d}\sigma.$$

Given $\phi \in L^2(D)$, we define $\phi_m^\alpha \in L^2(D+m)$ as

$$\phi_m^\alpha(y) = \phi(y-m)e^{\mathrm{i}\alpha\cdot m}.$$

Then it is clear that

$$\mathcal{S}_D^\alpha[\phi] = \sum_{m\in\Lambda} \mathcal{S}_{D+m}[\phi_m^\alpha].$$

We can then decompose

$$\begin{aligned}\mathcal{S}_D^\alpha[\phi] &= \sum_{m\in I_r} \mathcal{S}_{D+m}[\phi_m^\alpha] + \int_{\partial D} \sum_{m\in\Lambda\setminus I_r} G(x-y-m)e^{\mathrm{i}\alpha\cdot m}\phi(y)\,\mathrm{d}\sigma \\ &= \mathcal{S}_{\mathcal{D}_\mathrm{f}}[\phi^\alpha] + \mathcal{R}^\alpha[\phi],\end{aligned}$$

where, in the operator norm, $\mathcal{R}^\alpha = o(1)$ as $r \to \infty$. From the Neumann series, we now have

$$(\mathcal{S}_D^\alpha)^{-1}[\chi_{\partial D_i}] = \mathcal{S}_{\mathcal{D}_\mathrm{f}}^{-1}[\chi_i^\alpha] + o(1), \tag{2.8}$$

where χ_i^α is defined as

$$\chi_i^\alpha = \sum_{m\in I_r} \chi_{\partial D_i^m} e^{\mathrm{i}\alpha\cdot m}.$$

From Lemma B.2 in Appendix B, we know that the error term in (2.8) holds uniformly in α. If $m, n \in I_r$ are fixed and $i, j = 1, ..., N$, we then have from (2.8) that

$$\begin{aligned}C_{ij}^{m-n} &= \frac{1}{|Y^*|}\int_{Y^*}\int_{\partial D_i} e^{-\mathrm{i}\alpha\cdot(m-n)}\mathcal{S}_{\mathcal{D}_\mathrm{f}}^{-1}[\chi_j^\alpha]\,\mathrm{d}\sigma\,\mathrm{d}\alpha + o(1) \\ &= \int_{\partial D_i^m} \mathcal{S}_{\mathcal{D}_\mathrm{f}}^{-1}[\chi_{\partial D_j^n}]\,\mathrm{d}\sigma + o(1) \\ &= (C_\mathrm{f}^{mn})_{ij}(r) + o(1).\end{aligned}$$

This proves the claim. □

The numerical results presented in Figure 3 demonstrate the convergence of the capacitance coefficients, as established by Theorem 2.2. We plot $|(C_f)_{11}^0 - C_{11}^0|$ for both a one-dimensional and a two-dimensional lattice and show that this error converges algebraically to zero as the size of the finite lattice increases.

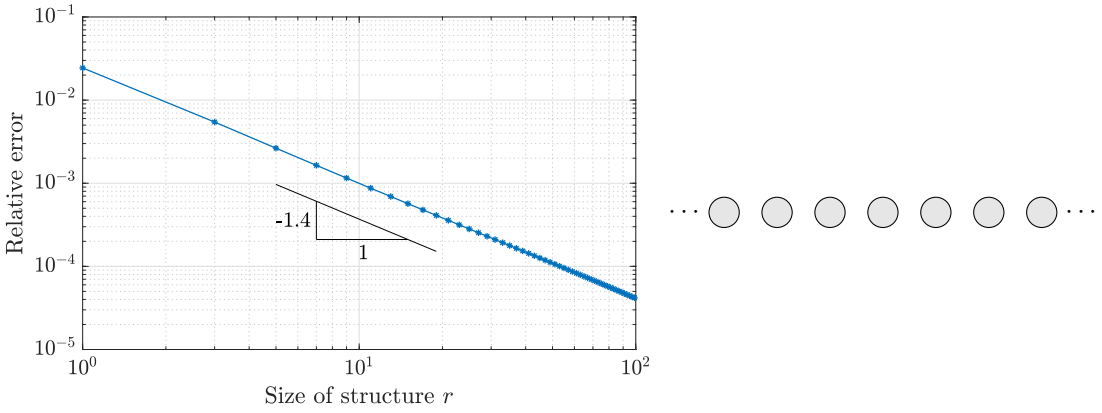

(a) One-dimensional lattice

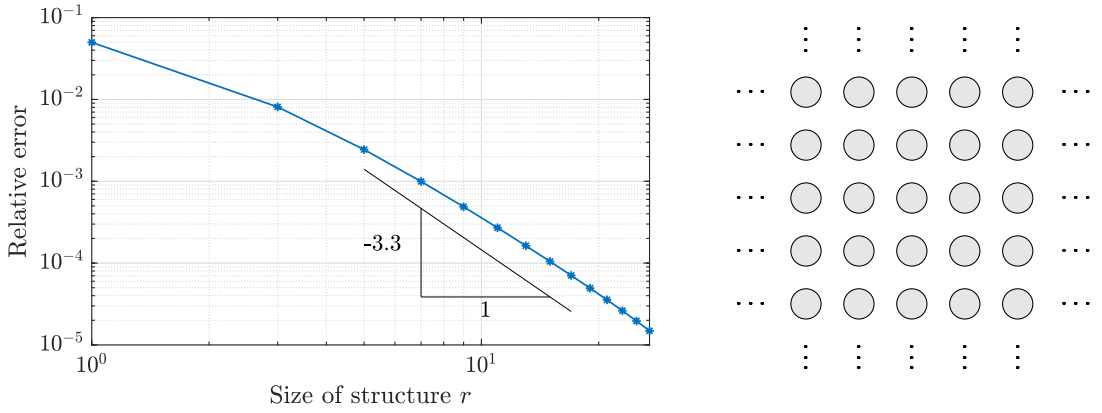

(b) Two-dimensional square lattice

Figure 3: Convergence of the capacitance coefficient of large finite lattices. (a) A one-dimensional lattice with a single resonator in the unit cell ($N = 1$). (b) A two-dimensional lattice with a single resonator in the unit cell ($N = 1$). In both cases, we plot $|(C_f)^0_{11} - C^0_{11}|$ for increasing numbers of resonators r. Here, the error scales as $O(r^{-3.3})$ for sufficiently small r.

3 Convergence to pure point spectrum

In this section, we study a problem where the infinite structure has a pure point spectrum, corresponding to a localized mode. We introduce a defect to the model in order to create such a mode. For a finite, truncated structure, there will be an eigenvalue arbitrarily close to the pure point spectrum.

3.1 Example of a defect structure

Before developing any convergence theory, we present an example of a defect structure exhibiting a pure point spectrum, corresponding to a localized mode. We take a lattice with a single resonator $N = 1$ inside each unit cell. We take a single resonator with perturbed ("defect") material parameter. In other words,

$$b_1^m = \begin{cases} 1, & m \neq 0, \\ 1 + x, & m = 0, \end{cases} \tag{3.1}$$

for some parameter $x > -1$. The eigenvalues of the (infinite-dimensional) generalized capacitance matrix $\mathfrak{BC}$ in this setting was studied in [2]. It was found that λ is an eigenvalue of $\mathfrak{BC}$ if and only if it is a root of the equation

$$\frac{x}{|Y^*|} \int_{Y^*} \frac{\lambda_1^\alpha}{\lambda - \lambda_1^\alpha} \, \mathrm{d}\alpha = 1, \tag{3.2}$$

where λ_1^α is the single eigenvalue of the quasi-periodic capacitance matrix $\widehat{C}^\alpha$ of the unperturbed periodic structure. This equation has a solution $\lambda = \lambda_0$ precisely in the case $x > 0$. In other words, the

defect induces an eigenvalue λ_0 in the pure point spectrum of $\mathfrak{BC}$, corresponding to an exponentially localized eigenmode. An example of such a localized eigenmode was shown in Figure 2.

3.2 Convergence of defect modes

In this section, we prove that, if the infinite structure has a localized mode, there will be an eigenvalue of the truncated structure arbitrarily close to the localized frequency.

We let $\mathfrak{C}$ denote the infinite capacitance matrix. As before, we let C_f denote the capacitance matrix of a finite structure of size $N|I_r| \times N|I_r|$. Furthermore, we let C_t denote the truncated matrix of $\mathfrak{C}$ of size $N|I_r| \times N|I_r|$, and similarly let B_t be the truncation of $\mathfrak{B}$. At this point, we emphasize that C_t is "nonphysical" in the sense that it does not correspond to a capacitance matrix associated to any physical structure but, rather, to the finite matrix obtained by simply truncating the infinite matrix $\mathfrak{C}$.

We assume that $\mathfrak{BC}$ has a localized eigenmode $\mathfrak{u}$, and let u_t be the truncation of $\mathfrak{u}$ of size $N|I_r|$. The first result follows only from the decay of the localized mode.

Lemma 3.1. *Assume that $\mathfrak{B}$ is a compact perturbation of the identity, such that $\mathfrak{BC}$ has a localized eigenmode $\mathfrak{u}$ with corresponding eigenvalue λ. Then there is an eigenvalue $\tilde{\lambda} = \tilde{\lambda}(r)$ of $B_\mathrm{t}C_\mathrm{t}$ satisfying*

$$\lim_{r\to\infty} \tilde{\lambda}(r) = \lambda.$$

Proof. We let $\mathfrak{u}_\mathrm{t}$ be the infinite vector obtained by padding u_t with 0. Since $\mathfrak{u}$ is in $\ell^2(\Lambda)$, for any $\varepsilon > 0$ we can choose large enough r so that

$$\|\mathfrak{u} - \mathfrak{u}_\mathrm{t}\|_{\ell^2} < \varepsilon.$$

Since $\mathfrak{BC}$ is a bounded operator, we then have

$$\|\lambda\mathfrak{u} - \mathfrak{BC}\mathfrak{u}_\mathrm{t}\|_{\ell^2} < K\varepsilon,$$

for some $K > 0$. Restricting to the finite block of size r, we have

$$\|\lambda u_\mathrm{t} - B_\mathrm{t}C_\mathrm{t}u_\mathrm{t}\|_2 < K\varepsilon.$$

In other words, λ is in the $K\varepsilon$-pseudospectrum of $B_\mathrm{t}C_\mathrm{t}$, and since $B_\mathrm{t}C_\mathrm{t}$ is normal, we have an eigenvalue $\tilde{\lambda}$ of $B_\mathrm{t}C_\mathrm{t}$ satisfying

$$|\tilde{\lambda}(r) - \lambda| = K\varepsilon.$$

This proves the claim. □

Next, we study the properties of C_f as the size of the finite structure increases.

Lemma 3.2. *For $i = 1, ..., N+1$, assume that $B_i \subset \mathbb{R}^3$ are disjoint, connected domains and let*

$$B = \bigcup_{n=1}^{N} B_i \quad \widetilde{B} = \bigcup_{n=1}^{N+1} B_i.$$

Let C_{ij}, $\widetilde{C}_{ij}$ denote the capacitance coefficients associated to B and $\widetilde{B}$, respectively. Then

$$C_{ii} \leq \widetilde{C}_{ii} \quad i = 1, ..., N.$$

Proof. We will use a variational characterization of the capacitance coefficients. Let $\mathcal{H} = \{v \in H^1_{\mathrm{loc}}(\mathbb{R}^3) \mid v(x) \sim |x|^{-1} \text{ as } x \to \infty\}$ and let

$$\mathcal{V} = \{v \in \mathcal{H} \mid v|_{\partial B_j} = \delta_{ij} \text{ for } j = 1, ..., N\},$$
$$\widetilde{\mathcal{V}} = \{v \in \mathcal{H} \mid v|_{\partial B_j} = \delta_{ij} \text{ for } j = 1, ..., N+1\}.$$

Observe that $\widetilde{\mathcal{V}} \subset \mathcal{V}$. It then follows that

$$C_{ii} = \min_{v\in\mathcal{V}} \int_{\mathbb{R}^3} |\nabla v|^2 \,\mathrm{d}x \leq \min_{v\in\widetilde{\mathcal{V}}} \int_{\mathbb{R}^3} |\nabla v|^2 \,\mathrm{d}x = \widetilde{C}_{ii}.$$

□

Remark 3.3. Lemma 3.2 states that the diagonal capacitance coefficients will always increase when adding additional resonators. In the physical situation of electrostatics this result is intuitive: the self-capacitance of a conductor can only increase if additional conductors are introduced.

Lemma 3.4. *As $r \to \infty$, we have $\|C_\mathrm{f}\|_2 < K$ for some K independent of r.*

Proof. We know that the capacitance matrix C_f is diagonally dominant:

$$(C_\mathrm{f}^{mm})_{ii} > \sum_{n\in\mathbb{Z},j\neq i} \big|(C_\mathrm{f}^{mn})_{ij}\big|,$$

for any i, m. For fixed i and m, we know from Lemma 3.2 that $(C_\mathrm{f}^{mm})_{ii}(r)$ is increasing in r, and for all r we have

$$(C_\mathrm{f}^{mm})_{ii}(r) < C_{ii}^0,$$

where, as before, C_{ii}^0 is the corresponding entry of the infinite capacitance matrix $\mathfrak{C}$. In particular, the eigenvalues of $C_\mathrm{f}(r)$ are bounded as $r \to \infty$, which shows the claim. □

As discussed above, the matrix C_t appearing in Lemma 3.1 is nonphysical, as it is a truncation of the matrix for the infinite system. Instead, we need to phrase the result for the matrix C_f, which describes the finite system. The following theorem is the main result of this section.

Theorem 3.5. *Assume that $\mathfrak{B}$ is a compact perturbation of the identity, such that $\mathfrak{BC}$ has a localized eigenmode $\mathfrak{u}$ with corresponding eigenvalue λ. Then there is an eigenvalue $\hat{\lambda} = \hat{\lambda}(r)$ of $B_\mathrm{t}C_\mathrm{f}$ satisfying*

$$\lim_{r\to\infty} \hat{\lambda}(r) = \lambda.$$

Proof. We let

$$K_1 = \sup_{r>0} \|C_\mathrm{f}(r) - C_\mathrm{t}\|_2,$$

and observe from Lemma 3.4 that $K < \infty$. We also let

$$K_2 = \|B_\mathrm{f}\|_2.$$

Given $\varepsilon > 0$, we pick $r_0 > 0$ such that the following four terms are small:

$$\|C_{0,\mathrm{f}} - C_{0,\mathrm{t}}\|_2 < \frac{\varepsilon}{4K_2}, \quad \|u_\mathrm{t} - u_{0,\mathrm{t}}\|_2 < \frac{\varepsilon}{4K_1K_2}, \quad \|B_\mathrm{f}(C_\mathrm{t} - C_{0,\mathrm{t}})u_{0,\mathrm{t}}\|_2 < \frac{\varepsilon}{4}, \quad \|B_\mathrm{f}(C_\mathrm{f} - C_{0,\mathrm{f}})u_{0,\mathrm{t}}\|_2 < \frac{\varepsilon}{4}$$

for all r large enough; the first inequality follows from Theorem 2.2 while the subsequent inequalities follow from the $\ell^2(\Lambda)$-decay of u. Here, $C_{0,\mathrm{t}}, u_{0,\mathrm{t}}$, and $C_{0,\mathrm{f}}$ are the truncations of $C_\mathrm{t}, u_\mathrm{t}$, and C_f to the smaller lattice of radius r_0 (padded with zero where needed for the matrix operations). We know from Lemma 3.1 that we can take r large enough so that $B_\mathrm{t}C_\mathrm{t}$ has an eigenvalue $\tilde{\lambda}$ of distance ε from λ. We then have

$$\begin{aligned} B_\mathrm{f}C_\mathrm{f}u_\mathrm{t} = B_\mathrm{f}C_\mathrm{t}u_\mathrm{t} + B_\mathrm{f}(C_\mathrm{f} - C_\mathrm{t})(u_\mathrm{t} - u_{0,\mathrm{t}}) + B_\mathrm{f}(C_{0,\mathrm{f}} - C_{0,\mathrm{t}})u_{0,\mathrm{t}} \\ + B_\mathrm{f}(C_\mathrm{f} - C_{0,\mathrm{f}})u_{0,\mathrm{t}} - B_\mathrm{f}(C_\mathrm{t} - C_{0,\mathrm{t}})u_{0,\mathrm{t}}. \quad (3.3) \end{aligned}$$

Then

$$\|(B_\mathrm{t}C_\mathrm{f} - B_\mathrm{t}C_\mathrm{t})u_\mathrm{t}\|_2 < \varepsilon,$$

which means that there is an eigenvalue $\hat{\lambda}$ of distance ε from $\widetilde{\lambda}$, and hence $|\hat{\lambda} - \lambda| < 2\varepsilon$. □

Remark 3.6. As an example, $\mathfrak{B}$ and $\mathfrak{C}$ as given in Section 3.1 satisfy the assumptions of Theorem 3.5.

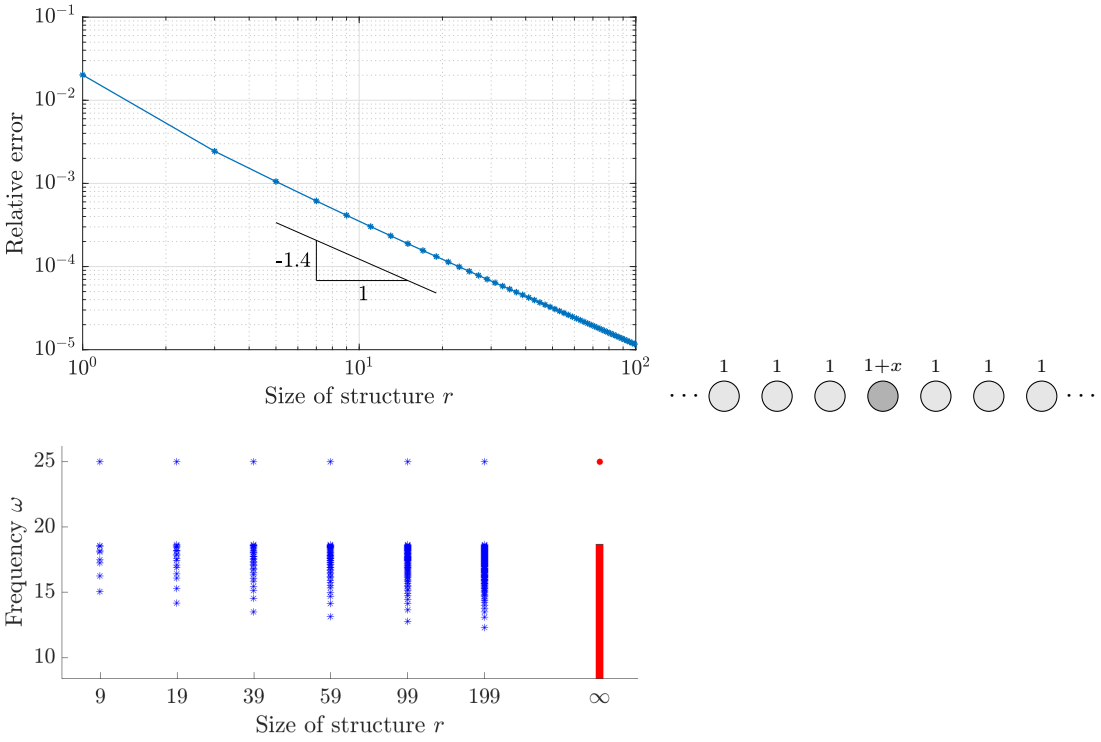

(a) One-dimensional lattice

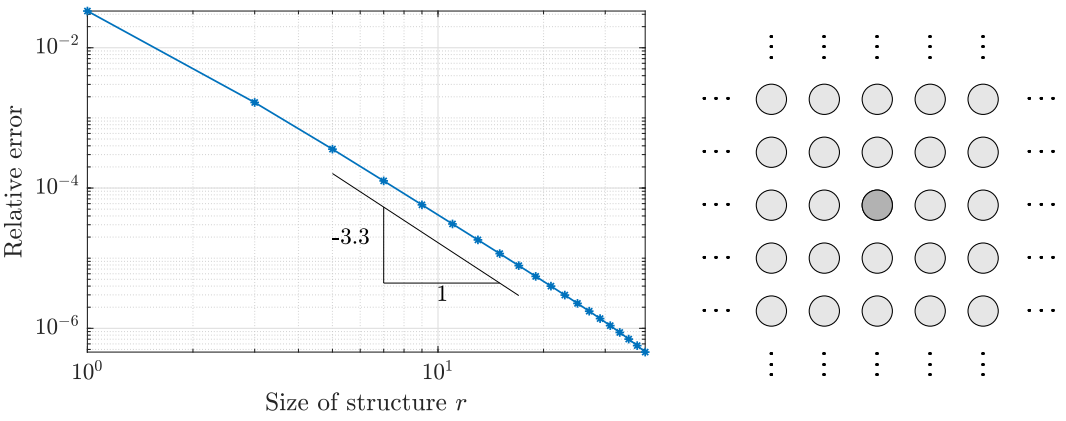

(b) Two-dimensional square lattice

Figure 4: Convergence of the frequency of the defect modes, for a defect on the central resonator (with $x = 1$) created by perturbing a single entry of $\mathfrak{B}$. (a) A one-dimensional lattice with a single resonator in the unit cell ($N = 1$). Here, the difference between the defect frequency computed for a finite structure and for the corresponding infinite structure scales as $O(r^{-1.4})$, where r is the length of the truncated structure. This is shown in the upper plot. The lower plot shows the spectrum of successively larger lattices. The defect frequency for the infinite structure is computed using (3.2). In the geometry sketch on the right, the corresponding entry b_1^m from the matrix $\mathfrak{B}$ is shown above each resonator. (b) A two-dimensional square lattice with a single resonator in the unit cell ($N = 1$). Here, the error scales as $O(r^{-3.3})$, where r is the width of the (square) truncated structure.

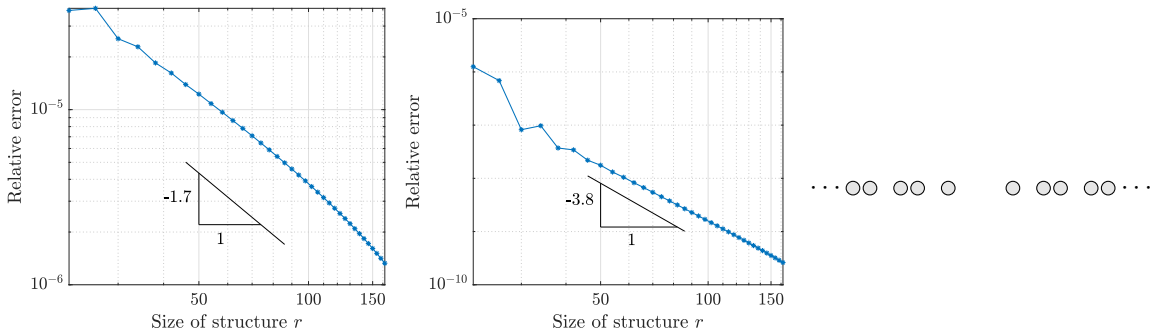

Figure 5: Convergence of the frequency of the defect modes in a lattice with resonators arranged in pairs ($N = 2$) and a defect corresponding to the two central resonators being removed. This gives two topologically protected edge modes. Here, the error scales as $O(r^{-1.7})$ for the even mode and $O(r^{-3.8})$ for the odd mode, where r is the length of the truncated structure.

3.3 Numerical illustration

Figure 4 shows the convergence of the difference between the defect frequency computed for a finite structure and for the corresponding infinite structure, computed analytically using *e.g.* (3.2). It is evident that the frequency converges algebraically, unlike related work on one-dimensional systems where the truncated frequency converges exponentially as a function of the length of the finite structure [14]. This holds irrespective of the dimensionality $d \in \{1, 2, 3\}$ of the lattice: the results in Figure 4a are for a one-dimensional lattice while Figure 4b shows a two-dimensional square lattice.

The reason for the algebraic convergence observed in this matrix model is the presence of long-range interactions between the coupled resonators (which scale inversely with the distance between resonators) and the fact that the capacitance matrix has all non-zero entries. Conversely, the exponential convergence observed in one-dimensional models, *e.g.* by [13, 14, 16], is due to the fact that the corresponding capacitance matrix is tridiagonal in this case [9]. It can be shown that the exponential convergence is a general property of tridiagonal matrix systems, whereas the algebraic convergence observed here is typical of three-dimensional scattering problems, where interactions scale inversely with distances.

Remark 3.7. Comparing Figure 4a and Figure 3a, it appears that the error of the frequency of the defect mode is inheriting the $O(r^{-1.4})$ convergence of the capacitance coefficients. Similar behaviour is observed for the square lattice, whereby $O(r^{-3.3})$ convergence is observed both for the defect mode in Figure 4b and the capacitance coefficient in Figure 3b. While this is unsurprising, it turns out not to be the case for other types of compact defect. For example, in Figure 5 we show the convergence of the defect modes in a dislocated Su-Schrieffer-Heeger (SSH) lattice, which is a one-dimensional lattice of resonators arranged in pairs (so $N = 2$). This system supports two defect modes that are known to be *topologically protected* and benefit from enhanced robustness properties (see [3] for details). The even mode experiences $O(r^{-1.7})$ convergence while the odd mode converges at a faster $O(r^{-3.8})$ rate. Understanding these different convergence rates is a valuable question for future study.

4 Convergence to continuous spectrum

Through numerical illustrations, we can illustrate how the discrete spectrum of the truncated structure approximates the Floquet-Bloch spectral bands of the infinite structure. Making analytic statements relating these two quantities, however, is a challenging problem that is beyond the scope of the present work. The two spectra have very different fundamental characteristics and a greater understanding of the edge effects that occur at the ends of the finite structure would be needed in order to make progress on this fiendish question.

We now outline the method used to compute the discrete band structure which, given the set of eigenpairs (ω_j, u_j) of a truncated structure, approximates the band structure of the periodic structure. If we take the size r of the truncated structure to be reasonably large, the eigenmode u_j will *approximately* be a linear combination of Bloch modes with frequency ω_j. To compare the discrete

eigenvalues of the truncated problem to the continuous spectrum of the periodic problem, we 'reverse engineer' the appropriate quasi-periodicities α corresponding to these Bloch modes. Observe that u_j is a vector of length $N|I_r|$. If we let $(u_j)_m$ denote the vector of length N associated to cell $m \in \Lambda$, we define the truncated Floquet transform of u_j as

$$(\hat{u}_j)_\alpha = \sum_{m \in I_r} (u_j)_m e^{\mathrm{i}\alpha \cdot m}, \qquad \alpha \in Y^*. \tag{4.1}$$

Observe that $(\hat{u}_j)_\alpha$ is a vector of length N. Looking at the 2-norm $\|(\hat{u}_j)_\alpha\|_2$ as a function of α, this function has distinct peaks at certain values of α. We then take the quasi-periodicitiy associated to the mode u_j as

$$\operatorname*{argmax}_{\alpha \in Y^*} \|(\hat{u}_j)_\alpha\|_2. \tag{4.2}$$

Note that the symmetry of the problem means that if α is an approximate quasi-periodicity then so will $-\alpha$ be. In cases of additional symmetries of the lattice, we expect additional symmetries of the quasi-periodicities.

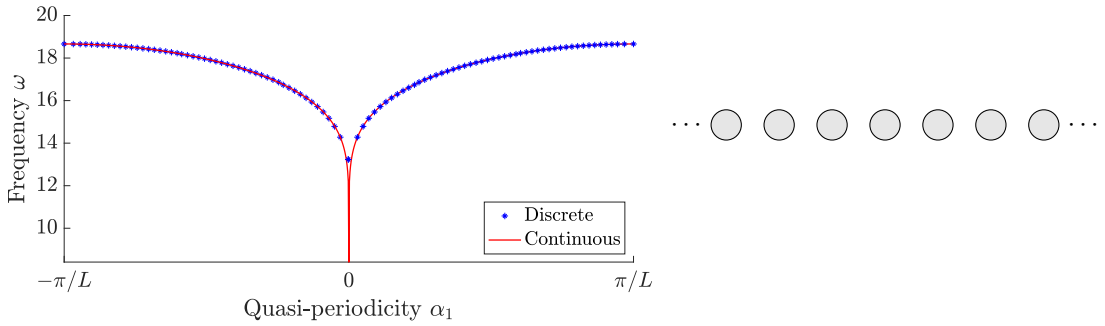

(a) Single periodic resonators ($N = 1$)

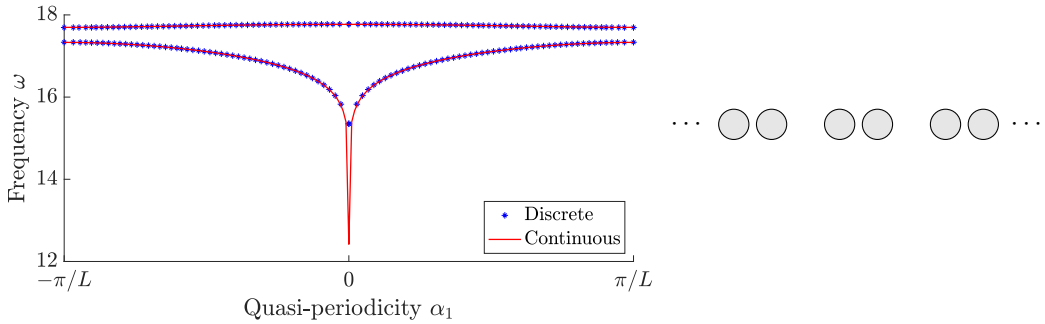

(b) Periodic pairs of resonators ($N = 2$)

Figure 6: The continuous spectrum of the infinite structure and the discrete spectrum of the truncated structure for a one-dimensional lattices. (a) Single periodic resonators ($N = 1$) with a truncated structure consisting of 50 resonators. (b) Periodic pairs of resonators ($N = 2$) with a truncated structure containing 100 resonators. In both cases, the truncated Floquet transform (4.1) *is used to approximate the quasi-periodicity of the truncated modes.*

Figure 6a shows the subwavelength continuous spectrum of an infinite array of resonators, which takes the form of a single spectral band. It is plotted alongside the discrete spectrum of a truncated array of 50 resonators, for which the quasi-periodicities have been approximated using the method outlined above. The discrete band structure mostly follows closely the infinite one, even for this relatively small truncated array. The frequencies close to zero are not exhibited in the finite structure, as the edge effects have the greatest effect on low-frequency modes. We would need to consider a much larger truncated structure to capture the lowest frequency part of the spectrum.

This behaviour can also be observed in more complicated structures. In Figure 6b, we compare the continuous and truncated spectra of an array of resonators arranged in pairs (dimers). The truncated structure has 100 resonators arranged in 50 pairs. This geometry is an example of the famous SSH

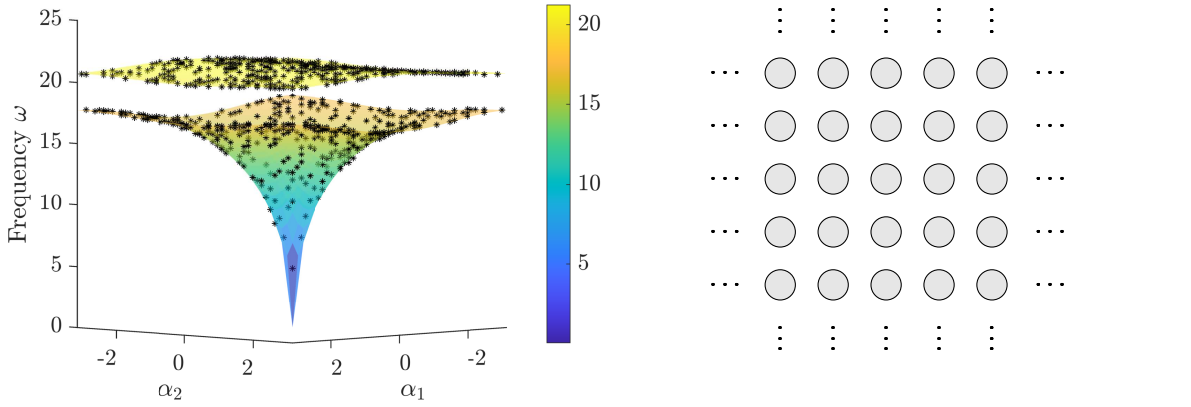

(a) Square lattice

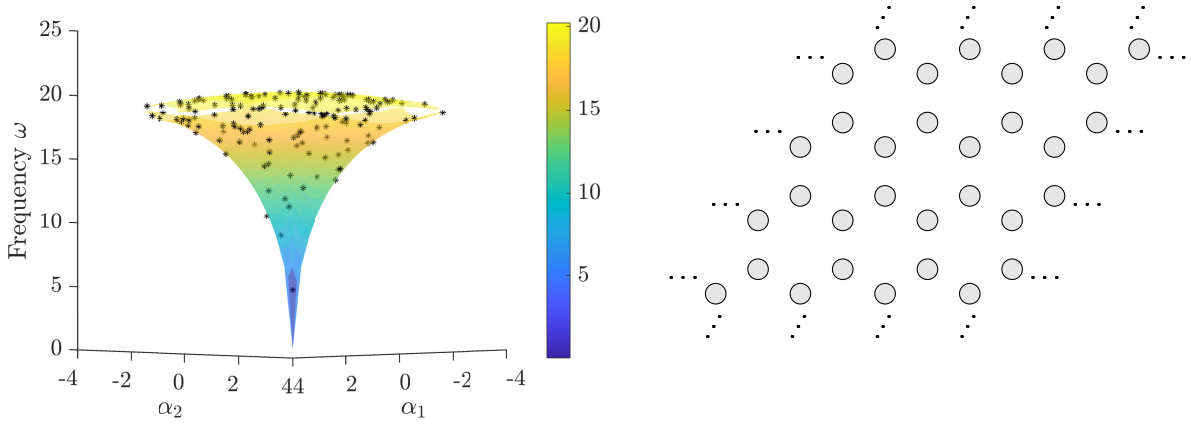

(b) Honeycomb lattice

Figure 7: Examples of continuous and discrete spectra of the infinite and truncated structures, respectively. (a) A square lattice with two resonators per unit cell, resulting in two bands separated by a gap. (b) A honeycomb lattice with Dirac cones at the vertices of the Brillouin zone. In both cases, the truncated structure have 800 resonators and the truncated Floquet transform is used to approximate the quasi-periodicity of the truncated modes.

chain [17] which has been shown to have fascinating topological properties [5]. This system has two subwavelength spectral bands and the truncated modes are split between approximating the two bands.

Additionally, we can consider this method for lattices of higher dimension. Figure 7a shows the case of a square lattice of resonator dimers. Similarly to Figure 6b, there is a band gap between the first and the second bands, and we see a close agreement between the discrete and the continuous band structure. Figure 7b shows a similar figure in the case of a honeycomb lattice, where the finite lattice is truncated along zig-zag edges of the lattice. As shown in [6], there are Dirac cones on each corner of the Brillouin zone. In the truncated structure, in addition to the "bulk modes" whose frequencies closely agree with the continuous spectrum, there are "edge modes" which are localized around the edges and whose points in the band structure lie away from the continuous bands.

5 Concluding remarks

In this work, we have demonstrated the convergence of defect modes in large resonator arrays to the corresponding modes in the infinite, periodic structure. We have studied this using the generalized capacitance matrix, which is a canonical model for three-dimensional wave scattering by resonant systems with long-range interactions. Our conclusions could also be generalized to other models, since the decay of the Helmholtz Green's function is the key feature that underpins our results. In

particular, the long-range "$1/r$" decay is the cause of the algebraic convergence we observe, in contrast to the exponential convergence observed in analogous one-dimensional settings.

A significant advantage of the model used in this work is that the Bloch modes, in addition to the defect modes, are also concisely characterized. As detailed in Section 4, this provides a numerical method for approximating the continuous spectrum. Importantly, this constructive approach presents a possible avenue for proving statements about the convergence of eigenvalues to the continuous spectrum. We see developing this convergence theory as a challenging but important problem for future investigation. Even in one-dimensional models, demonstrating convergence to the continuous spectrum remains an open problem.

Data availability

No new data were created or analyzed in this study.

A Asymptotic derivation of the model

In this brief appendix, we recall how the generalized capacitance matrix arises through an asymptotic treatment of a system of coupled high-contrast resonators. In particular, it can be used to characterize the subwavelength (*i.e.* asymptotically low-frequency) resonance of the system. For more details and a review of extensions to other settings (such as non-Hermitian and time-modulated systems) see [1].

We will present the results for a finite system of resonators. Analogous results hold for infinite periodic systems, by modifying the Green's function appropriately [1]. We suppose that the material inclusions $D_i \subset \mathbb{R}^3$, as considered already in this work, represent the material inclusions that will act as our resonators. We consider the scattering of time-harmonic waves with frequency ω and will solve a Helmholtz scattering problem in three dimensions. This Helmholtz problem, which can be used to model acoustic, elastic and polarized electromagnetic waves, represents the simplest model for wave propagation that still exhibits the rich phenomena associated to subwavelength physics.

We use v_i denote the wave speed in each resonator D_i. In which case, $k_i = \omega/v_i$ is the wave number in D_i. Similarly, the wave speed and wave number in the background medium are denoted by v and k. Finally, we must introduce the material contrast parameters $\delta_1, \dots, \delta_N$. These parameters describe the contrast between the material inside D_i and the background material. For example, in the case of an acoustic system, δ_i is the density of the material inside D_i divided by the density of the background material. We will want these contrast parameters to be small (an air bubble in water is one famous example in the setting of acoustics). Then for the domain

$$D = \bigcup_{m \in I_r} \bigcup_{i=1}^{N} (D_i + m),$$

we consider the Helmholtz resonance problem

$$\begin{cases} \Delta u + k^2 u = 0 & \text{in } \mathbb{R}^d \setminus \overline{D}, \\ \Delta u + k_i^2 u = 0 & \text{in } D_i + m, \text{ for } i = 1, \dots, N, \ m \in I_r, \\ u|_+ - u|_- = 0 & \text{on } \partial D, \\ \delta_i \dfrac{\partial u}{\partial \nu}\Big|_+ - \dfrac{\partial u}{\partial \nu}\Big|_- = 0 & \text{on } \partial D_i + m \text{ for } i = 1, \dots, N, \ m \in I_r, \\ u(x) \text{ satisfies the Sommerfeld radiation condition,} \end{cases} \tag{A.1}$$

where the Sommerfeld radiation condition says that

$$\lim_{|x| \to \infty} |x|^{\frac{d-1}{2}} \left(\frac{\partial}{\partial |x|} - \mathrm{i}k \right) u = 0, \quad \text{uniformly in all directions } x/|x|, \tag{A.2}$$

and guarantees that energy is radiated outwards by the scattered solution.

The asymptotic regime we consider is that the material contrast parameters are all small while the wave speeds are all of order one. That is, there exists some $\delta > 0$ such that

$$\delta_i = O(\delta) \quad \text{and} \quad v, v_i = O(1) \quad \text{as} \quad \delta \to 0, \text{ for } i = 1, \dots, N. \tag{A.3}$$

Within this setting, we are interested in solutions to the resonance problem (A.1) that are *subwavelength* in the sense that

$$\omega \to 0 \quad \text{as} \quad \delta \to 0. \tag{A.4}$$

To be able to characterize the subwavelength resonant modes of this system, we must define the *generalized* capacitance coefficients. Recall the capacitance coefficients $(C_{\mathrm{f}}^{mn})_{ij}$ from (2.1). Then, we define the corresponding generalized capacitance coefficient as

$$(\mathcal{C}_{\mathrm{f}}^{mn})_{ij} = \frac{\delta_i v_i^2}{|D_i^m|}(C_{\mathrm{f}}^{mn})_{ij}, \tag{A.5}$$

where $|D_i^m|$ is the volume of the bounded subset D_i^m. Then, the eigenvalues of $\mathcal{C}_{\mathrm{f}}$ determine the subwavelength resonant frequencies of the system, as prescribed by the following theorem.

Theorem A.1. *Consider a system of $N|I_r|$ subwavelength resonators in $\mathbb{R}^3$. For sufficiently small $\delta > 0$, there exist $N|I_r|$ subwavelength resonant frequencies $\omega_1(\delta), \ldots, \omega_{N|I_r|}(\delta)$ with non-negative real parts. Further, the subwavelength resonant frequencies are given by*

$$\omega_n = \sqrt{\lambda_n} + O(\delta) \quad \textit{as} \quad \delta \to 0,$$

where $\{\lambda_n : n = 1, \ldots, N|I_r|\}$ are the eigenvalues of the generalized capacitance matrix $\mathcal{C}_{\mathrm{f}}$, which satisfy $\lambda_n = O(\delta)$ as $\delta \to 0$.

A similar result exists for an infinite periodic structure, in terms of the eigenvalues of the *generalized* quasi-periodic capacitance matrix, as defined in (2.4), see [1] for details.

The definition (A.5) clarifies the motivation for pre-multiplying by the perturbation matrix $\mathfrak{B}$ to describe defects. When $\mathfrak{B}$ is a compact perturbation of the identity, it describes defects that correspond to changing the material parameters on a finite number of resonators, so that the quantity $\delta_i v_i^2$ corresponding to those resonators is altered.

B Uniformity across the Brillouin zone

In this appendix, we provide additional details of the proof of Theorem 2.2. The main result is Lemma B.2, which shows that $(\mathcal{S}_D^\alpha)^{-1}$ is in operator norm, uniformly bounded for α in a neighbourhood of 0. The analysis is similar to [4, Section 3.3].

From *e.g.* [7], we have a dual-space representation of G^α given by

$$G^\alpha(x) = -\frac{1}{|Y|}\sum_{q\in\Lambda^*}\frac{e^{\mathrm{i}(\alpha+q)\cdot x}}{|\alpha+q|^2} = \frac{-e^{\mathrm{i}\alpha\cdot x}}{|Y||\alpha|^2} - \frac{1}{|Y|}\sum_{q\in\Lambda^*\setminus\{0\}}\frac{e^{\mathrm{i}(\alpha+q)\cdot x}}{|\alpha+q|^2}.$$

Define the periodic Green's function G^0 as

$$G^0(x) = -\frac{1}{|Y|}\sum_{q\in\Lambda^*\setminus\{0\}}\frac{e^{\mathrm{i}q\cdot x}}{|q|^2}.$$

For α close to zero, we then have

$$G^\alpha(x) = \frac{-1}{|Y||\alpha|^2} - \frac{\mathrm{i}\alpha\cdot x}{|Y||\alpha|^2} + \frac{(\alpha\cdot x)^2}{2|Y||\alpha|^2} + G^0(x) + O(|\alpha|).$$

Consequently, for α close to zero, we have the an expansion of the single-layer potential $\mathcal{S}_D^\alpha$:

$$\begin{aligned}\mathcal{S}_D^\alpha[\psi](x) = -\frac{1}{|Y||\alpha|^2}\int_{\partial D}\psi(y)\,\mathrm{d}\sigma - \frac{\mathrm{i}}{|Y||\alpha|^2}\int_{\partial D}\alpha\cdot(x-y)\psi(y)\,\mathrm{d}\sigma \\ + \frac{1}{2|Y||\alpha|^2}\int_{\partial D}\big(\alpha\cdot(x-y)\big)^2\psi(y)\,\mathrm{d}\sigma + \mathcal{S}_D^0[\psi](x) + O(|\alpha|).\end{aligned} \tag{B.1}$$

Lemma B.1. *If $\mathcal{S}_D^0[\varphi] = K\chi_{\partial D}$ for some constant K and some $\varphi \in L^2(\partial D)$ satisfying $\int_{\partial D}\varphi\,\mathrm{d}\sigma = 0$, then $\varphi = 0$.*

Proof. For $x \in \mathbb{R}^3 \setminus \mathcal{D}$, define $V(x) := \mathcal{S}_D^0[\varphi](x)$. Then V solves the following differential problem,

$$\begin{cases} \Delta V = 0 & \text{in } \mathbb{R}^3 \setminus \mathcal{D}, \\ V|_+ = K & \text{on } \partial\mathcal{D}, \\ V(x+m) = V(x) & \text{for all } m \in \Lambda. \end{cases} \tag{B.2}$$

Moreover, using the jump relations and integration by parts, we have that

$$\int_{\partial D} \varphi \, \mathrm{d}\sigma = K \int_{Y \setminus D} |\nabla V|^2 \, \mathrm{d}x = 0.$$

If $K \neq 0$, it follows from (B.2) that $\int_{Y\setminus D} |\nabla V|^2 \, \mathrm{d}x \neq 0$ which is a contradiction. In other words we must have $K = 0$, so that $\mathcal{S}_D^0[\varphi] = 0$ and $\int_{\partial D} \varphi \, \mathrm{d}\sigma = 0$. From [4, Lemma 3.7], we have that $\varphi = 0$. □

Lemma B.2. *$\|(\mathcal{S}_D^\alpha)^{-1}\|$, in operator norm, is bounded for α in a neighbourhood of 0.*

Proof. To reach a contradiction, we assume that $\mathcal{S}_D^\alpha[\phi] = O(|\alpha|)$ for some ϕ, which can be written as $\phi = \phi_0 + |\alpha|\phi_1$, where ϕ_0 is nonzero, does not depend on α, and $\phi_1 = O(1)$ as $|\alpha| \to 0$. Also define $\mathbf{v} = \frac{\alpha}{|\alpha|}$. From (B.1) it follows that

$$\begin{aligned} \int_{\partial D} \phi_0 \, \mathrm{d}\sigma &= 0, \\ \int_{\partial D} \phi_1(y) \, \mathrm{d}\sigma + \mathrm{i} \int_{\partial D} \mathbf{v} \cdot (x-y)\phi_0(y) \, \mathrm{d}\sigma &= O(|\alpha|), \\ K(\mathbf{v}) - \mathrm{i}\mathbf{v} \cdot x \int_{\partial D} \phi_1(y) \, \mathrm{d}\sigma + \frac{1}{2} \int_{\partial D} \big(\mathbf{v} \cdot (x-y)\big)^2 \phi_0(y) \, \mathrm{d}\sigma + |Y| \mathcal{S}_D^0[\phi_0] &= O(|\alpha|), \end{aligned}$$

where K is constant as function of x. Simplifying, we have that

$$\frac{1}{2} \int_{\partial D} \big(\mathbf{v} \cdot (x-y)\big)^2 \phi_0(y) \, \mathrm{d}\sigma = -(\mathbf{v} \cdot x) \int_{\partial D} (\mathbf{v} \cdot y)\phi_0(y) \, \mathrm{d}\sigma + \frac{1}{2} \int_{\partial D} (\mathbf{v} \cdot y)^2 \phi_0(y) \, \mathrm{d}\sigma.$$

In total we get

$$\mathcal{S}_D^0[\phi_0](x) = \tilde{K}(\mathbf{v}) + \frac{2(\mathbf{v} \cdot x)}{|Y|} \int_{\partial D} (\mathbf{v} \cdot y)\phi_0(y) \, \mathrm{d}\sigma,$$

where $\tilde{K}$ is constant in x. Observe that $\mathcal{S}_D^0[\phi_0](x)$ is independent of $\mathbf{v}$. As a function of x, this function is constant for $x \in \mathbf{v}^\perp$, and so this function is constant for all x. From Lemma B.1 we get that $\phi_0 = 0$ which proves the claim. □

References

[1] H. Ammari, B. Davies, and E. O. Hiltunen. Functional analytic methods for discrete approximations of subwavelength resonator systems. *arXiv preprint arXiv:2106.12301*, 2021.

[2] H. Ammari, B. Davies, and E. O. Hiltunen. Anderson localization in the subwavelength regime. *arXiv preprint arXiv:2205.13337*, 2022.

[3] H. Ammari, B. Davies, and E. O. Hiltunen. Robust edge modes in dislocated systems of subwavelength resonators. *J. London Math. Soc.*, 106(3):2075–2135, 2022.

[4] H. Ammari, B. Davies, E. O. Hiltunen, H. Lee, and S. Yu. Exceptional points in parity–time-symmetric subwavelength metamaterials. *SIAM J. Math. Anal.*, 54(6):6223–6253, 2022.

[5] H. Ammari, B. Davies, E. O. Hiltunen, and S. Yu. Topologically protected edge modes in one-dimensional chains of subwavelength resonators. *J. Math. Pures Appl.*, 144:17–49, 2020.

[6] H. Ammari, B. Fitzpatrick, E. O. Hiltunen, H. Lee, and S. Yu. Honeycomb-lattice Minnaert bubbles. *SIAM J. Math. Anal.*, 52(6):5441–5466, 2020.

[7] H. Ammari, H. Kang, and H. Lee. *Layer Potential Techniques in Spectral Analysis*, volume 153 of *Mathematical Surveys and Monographs*. American Mathematical Society, Providence, 2009.

[8] R. A. Diaz and W. J. Herrera. The positivity and other properties of the matrix of capacitance: Physical and mathematical implications. *J. Electrost.*, 69(6):587–595, 2011.

[9] F. Feppon, Z. Cheng, and H. Ammari. Subwavelength resonances in 1D high-contrast acoustic media. *HAL preprint hal-03697696*, 2022.

[10] N. L. Hills and S. N. Karp. Semi-infinite diffraction gratings – I. *Commun. Pure Appl. Math.*, 18:203–233, 1965.

[11] L. M. Joseph and R. V. Craster. Reflection from a semi-infinite stack of layers using homogenization. *Wave Motion*, 54:145–156, 2015.

[12] P. A. Kuchment. *Floquet Theory for Partial Differential Equations*, volume 60 of *Operator Theory: Advances and Applications*. Springer Science & Business Media, 1993.

[13] J. Lin. A perturbation approach for near bound-state resonances of photonic crystal with defect. *European J. Appl. Math.*, 27(1):66–86, 2016.

[14] J. Lin and F. Santosa. Resonances of a finite one-dimensional photonic crystal with a defect. *SIAM J. Appl. Math.*, 73(2):1002–1019, 2013.

[15] C. M. Linton, R. Porter, and I. Thompson. Scattering by a semi-infinite periodic array and the excitation of surface waves. *SIAM J. Appl. Math.*, 67(5):1233–1258, 2007.

[16] J. Lu, J. L. Marzuola, and A. B. Watson. Defect resonances of truncated crystal structures. *SIAM J. Appl. Math.*, 82(1):49–74, 2022.

[17] W. P. Su, J. R. Schrieffer, and A. J. Heeger. Solitons in polyacetylene. *Phys. Rev. Lett.*, 42:1698–1701, 1979.

[18] I. Thompson and R. I. Brougham. A direct method for Bloch wave excitation by scattering at the edge of a lattice. part i: Point scatterer problem. *Q. J. Mech. Appl. Math.*, 71(1):1–24, 2018.

[19] N. Tymis and I. Thompson. Scattering by a semi-infinite lattice and the excitation of Bloch waves. *Q. J. Mech. Appl. Math.*, 67(3):469–503, 2014.

[20] E. D. Vinogradova, K. Kobayashi, and T. Eizawa. Full wave analysis of plane wave diffraction by a finite sinusoidal grating: E-polarization case. *Wave Motion*, 86:44–62, 2019.